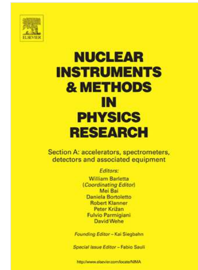

Light yield, long-term stability, and attenuation length of a new plastic scintillator cured at room temperature

E. Saito, H. Miyata, M. Katsumata, Y. Karasawa, T. Koike, H. Ono, M. Watanabe, M. Sato, A. Umeyama, T. Suzuki, M. Tamura

PII: S0168-9002(19)31302-6
DOI: https://doi.org/10.1016/j.nima.2019.162885
Reference: NIMA 162885

To appear in: *Nuclear Inst. and Methods in Physics Research, A*

Received date : 27 April 2019
Revised date : 27 September 2019
Accepted date : 28 September 2019

Light yield, long-term stability, and attenuation length of a new plastic scintillator cured at room temperature

E. Saito[a]*, H. Miyata[b], M. Katsumata[b,1], Y. Karasawa[b], T. Koike[a], H. Ono[c], M. Watanabe[c], M. Sato[d], A. Umeyama[d], T. Suzuki[d], M. Tamura[d]

[a] *Graduate School of Science and Technology, Niigata University, Niigata 950-2181, Japan*
[b] *Department of Physics, Faculty of Science, Niigata University, Niigata 950-2181, Japan*
[c] *The Nippon Dental University School of Life Dentistry at Niigata, Niigata 951-8580, Japan*
[d] *Carlit Holdings Co., Ltd., Chuo, Tokyo 104-0031, Japan*

* Corresponding author. Tel./fax: +81252626138.
E-mail: esaito@hep.sc.niigata-u.ac.jp (E. Saito), miyata@hep.sc.niigata-u.ac.jp (H. Miyata)
URL: http://www.hep.sc.niigata-u.ac.jp (E. Saito, H. Miyata)
[1] Present address: Kanagawa Prefectural Institute of Public Health, Chigasaki 253-0087, Japan

Abstract

We, in collaboration with Carlit Holdings Co., Ltd., developed a new plastic scintillator that can be cured at room temperature by mixing a base resin with a hardener solution. We evaluated the scintillator's characteristics of light yield, stability, and attenuation length using a ^{90}Sr β-ray source. The plastic scintillator showed 40% of the light yield of the commercially available scintillator BC408, or 26% of that of the standard organic scintillator anthracene. The long-term light stabilities of the plastic scintillators, with and without the doping stabilizer agent 2,6-di-*tert*-butyl-4-methylphenol (BHT), were measured for 6 months. The BHT-doped sample retained 80% of the initial light yield over this period. The initial attenuation length of 0.9 m was obtained. The new plastic scintillator showed good stability against oxidative environments, although improvements in its light yield and attenuation length could be achieved by further optimizing its component materials and processing.

Keywords: Plastic scintillator, Room-temperature curing resin, Light yield, Long-term stability, Attenuation length

1. Introduction

Scintillation counters have been used as radiation detectors in high-energy and nuclear physics for many years. They have recently been applied as beam monitors in medical treatment [1–3], nuclear reactors [4, 5], and environmental radiation monitors [6]. Solid plastic scintillators are more easily handled and processed into various forms than liquid scintillators; however, they are relatively expensive. As plastic scintillator technology has matured, studies have been conducted to reduce manufacturing cost [7], improve radiation tolerance [8], and enhance neutron sensitivity [9–11] in recent years. In addition, lower-cost plastic scintillators are preferred for developing large-size calorimeters in high-energy physics [12–14] and neutrino detectors for reactor monitoring experiments [15–17].

In several projects, gadolinium-doped liquid scintillators have been adopted for increased neutron sensitivity from their large cross-sections by achieving large volumes [18–20]. However, because liquid scintillators are composed of flammable oil, avoiding the placement of large volumes of liquid scintillators near nuclear power plants is preferred. From this perspective, we developed the lower-cost gadolinium-doped plastic scintillator to facilitate a large volume of approximately one cubic meter [21].

In this study, we measured the light yield, attenuation length, and long-term stability of the newly developed plastic scintillator cured at room temperature and compared these properties with those of the commercially available standard BC408 (Saint-Gobain Co.) plastic scintillator.

The new plastic scintillator is advantageous because room-temperature curing avoids the high-temperature processes required for standard commercial plastic scintillators, thus decreasing manufacturing costs and simplifying the facility requirements. In addition, freedom in shaping is increased because a broader variety of mold materials can be used. Furthermore, heat-labile functional materials can be added to improve the specific particle detection efficiency of the plastic scintillator.

2. Materials and methods

2.1. New manufacturing method

Standard commercial plastic scintillators are usually composed of polystyrene or polyvinyl toluene with wavelength shifters. 2,5-Diphenyloxazole (PPO) and 1,4-bis(2-methylstyryl)benzene (bis-MSB) are used as the primary and secondary wavelength shifters, respectively. When plastic scintillators are made by casting or extrusion methods, these materials are heated to about 100℃ or more [10]. After heating, plastic scintillators are cooled slowly to prevent cracking.

We have developed a new plastic scintillator in collaboration with Carlit Holdings Co., Ltd., with a focus on reducing the production cost. The new plastic scintillator uses a bisphenol A-type epoxy resin as the base material, which can be cured at room temperature by mixing with an amine-based curing agent containing wavelength shifters (PPO, bis-MSB) and an antioxidant agent. The density and refractive index of the new plastic scintillator are (1.15–1.16) ± 0.02 g/cm^3 and 1.60 ± 0.04 (for 450-nm laser light), respectively, almost equal to those of the standard BC408 scintillator, which has the density and refractive index of 1.032 g/cm^3 and 1.58, respectively [22].

In this study, we used different scintillator base materials and modified the manufacturing procedure from that used in a previous study [21] to improve the transparency and reduce the variation in the samples. In addition, we added the antioxidant agent of 2,6-di-*tert*-butyl-4-methylphenol (BHT) and performed a post-curing process of holding for 6 h at 58 °C after room-temperature curing in order to improve the stability of light yield and attenuation length. We measured the light yield and the stability thereof of the new scintillator samples compared to those of BC408. All tested new plastic scintillators were fabricated using base materials from the same manufacturing lots.

2.2. Experimental setup

The experimental setup for measuring the light yield is shown in Fig. 1. The plastic scintillator samples prepared for this study are summarized in Table 1. We prepared six types of 40 mm × 75 mm × 3 mm plastic scintillator samples for light yield measurement (Fig. 2). Each plastic scintillator sample was shaped with a silicone rubber mold to improve the shape accuracy and reduce cutting uncertainty. The silicone frame comprised a 3-mm-thick silicone rubber sheet that was die-cut to 75 mm × 40 mm. In addition, we applied an air bubble removal process for the sample scintillators after mixing the resin and hardener.

We prepared two scintillator samples for each type. The sample with better air bubble removal was named "-1" and the other was named "-2". As a reference, BC408 scintillators were also prepared with the same shape. Four sides of each sample scintillator plate were polished by an abrasive film and the 40 mm × 3 mm side was connected to a photomultiplier tube (PMT) using optical grease (BC630, Saint-Gobain Co.). During the measurement, each plastic scintillator was covered with an aluminized mylar sheet and a black sheet to increase the light yield and shield the scintillator from external light, respectively.

To select β-rays emitted from a ^{90}Sr β-ray source ($E_{\max}$ = 2.28 MeV, 1.7 MBq) that penetrated a 2-mm-diameter aluminum collimator of 10 mm in thickness and the sample scintillator, a trigger scintillator (BC408, 40 mm × 40 mm × 2 mm) was set under the sample scintillator (Fig. 1). The PMTs of the sample and trigger scintillation counters were closely confined in a black box.

In the experiment, the β-ray loses energy in the sample scintillator, releasing scintillation light. The scintillation light propagates through the scintillator and enters into a photocathode of the PMT (H7195, Hamamatsu Photonics K.K.) that is supplied with −2100 V. A signal charge from the PMT is converted to a digital signal by a charge-sensitive analog-to-digital converter (CSADC, V005, 14-bit, HOSHIN ELECTRONICS CO., LTD.). The ADC has the dynamic range 0–1000 pC and receives gate signals of 200 ns derived from the trigger scintillation counter. The irradiation position of the β-ray is located 6 cm from the PMT surface on the centerline in the length direction of the scintillator. Each measurement was 5 min in duration.

One of the most important objectives of this study is the investigation of the long-term stability of the light yield of the new plastic scintillators. Scintillator samples were placed in a shading bag when not being tested and stored in a desiccator with the average temperature of 19.2 °C. Seasonal variations of the temperature spanned 10.4 to 24.3 °C.

A motorized stage (position accuracy of ±15 μm, OSMS26-200(X), SIGMAKOKI CO., LTD.) was used for highly precise positioning of the β-ray source and trigger scintillation counter (Fig. 1).

3. Results

3.1. Stability of light yield

The pulse shapes of the sample plastic scintillators, as observed by an oscilloscope, are shown in Fig. 3. One scintillator is selected from the two samples of each type. The light signal of this scintillator under β-rays is observed and the average pulse shape is recorded.

As shown in Fig. 3, the pulse widths of the new plastic scintillators are similar to that of BC408 at approximately 10–20 ns. The light yield is evaluated as the signal pulse height (PH). The PH is calculated as the signal-mean subtracted from the pedestal-mean (Fig. 4). The seven graphs in Fig. 4 are acquired using samples with names ending in “-1”.

The mean values found from the histograms and the ratios of these mean values to the average mean value of BC408 are shown in Table 2. The mean values (ch/mm) are normalized by the sample scintillator thickness measured at the β-ray irradiation position using a micrometer to within an accuracy of 0.002 mm. The light yields of the new plastic scintillators are defined as the mean values (ch/mm) and are 33–46% of those for BC408. The light yields measured here are approximately two times higher than that in a previous study [21].

The long-term stability of the light yield is measured with results as shown in Fig. 5. The values of all data points are normalized by the initial value to evaluate the stability as a percentage. The data are plotted using two symbols to distinguish the two scintillator samples of each type. In Fig. 5, each sample pair was measured on almost same date and time. The error in the light yield measurements is estimated as the standard deviation of the results of the thirty measurements of BC408-1. The relative error is 2.6%.

As shown in Fig. 5, the light yield is generally stable for antioxidant-containing new scintillators. The influence of environmental oxidation is suppressed by the antioxidant. The light yield of the antioxidant-added new plastic scintillators maintains 80% of the initial value over at least 6 months. This indicates that the antioxidant stabilizes the new plastic scintillator.

3.2. Stability of attenuation length

The attenuation length of the scintillation light was measured [21, 23, 24]. The sample scintillator size was 20 mm × 200 mm × 3 mm, as in our previous study [21]. The most stable new plastic scintillator type, as shown in Fig. 5, is NGT6; therefore, the attenuation length of the NGT6L scintillator was measured and compared to that of the standard BC408L, which was cut from the BC408 scintillator plate. We added “-1” to the sample name of the one with fewer air bubbles and “-2” to the other. Four sides of each sample scintillator were polished using a grinder and one of the 20 mm × 3 mm sides was connected to a PMT using optical grease (BC630, Saint-Gobain Co.), as with the light yield measurement specimens in Table 1.

The method for measuring attenuation length was similar to that used previously [21], with the same setup as shown in Fig. 1. The irradiation position of the β-ray was 6 to 18 cm from the PMT surface. The detected light yield is defined as the mean value and normalized by the thickness at the irradiation position of the β-ray (Table 3). The scintillator samples were stored as described in section 2.2. The measurement results are shown in Fig. 6. The mean value of the light yield, which depends on the irradiation position, is fitted with equation (1):

$$f = \left(A + \frac{B}{x^2}\right) \cdot e^{-x/L}\ , \tag{1}$$

where A and B are amplitudes, x is the horizontal distance between the irradiation position and the PMT surface, and L is the light attenuation length [21]. In Fig. 6, the error in the light yield measurements is estimated as the standard deviation of five measured values from BC408L, as in the previous study [21]. The relative error is 1.3%. The standard deviation of the light yield in each data point is independent of the distance between the PMT surface and β-ray incident position and equal to 1.3%; this is attributed to errors in each data point in the attenuation length measurement. For the sample scintillators NGT6L-1,2, the first measurements are performed approximately one month after the demolding of the scintillators, while the last measurements are obtained about eight months later. For BC408L, the last measurement is performed one year after the first measurement.

The storage times of the sample scintillators at measurement and the results of the attenuation length measurements are shown in Table 4 and Fig. 7. In Fig. 7, the BC408L measurement day differs from that of NGT6L-1 and -2. NGT6L-1 is manufactured with a high-quality polishing process and has fewer air bubbles than NGT6L-2. The long-term stability of the attenuation length could be improved, although the NGT6L-1 scintillator showed the initial attenuation length of approximately 0.9 m. The specified attenuation length of BC408 is 2.1 m [22]. However, the BC408 sample used for the specification is large (1 cm × 20 cm × 200 cm), we measure a different initial attenuation length of 0.94 m.

4. Summary

We developed a new plastic scintillator using room-temperature-curable resin. The light yield of the new plastic scintillator was approximately 40% of that of the standard commercial BC408 and 26% of that of anthracene.

The light yield of the new plastic scintillator containing 1 wt% BHT (as an antioxidant) showed 80% maintenance of the initial value over 6 months storage. The scintillator stability was improved with both BHT and post-curing treatment for 6 h at 58 °C.

The measured attenuation length of the post-cured BHT-containing plastic scintillator was approximately 0.9 m. The long-term stability of the attenuation length requires improvement, which will be attempted in a future study.

To increase the light yield, attenuation length, and long-term stability of these properties, we plan to develop as follows. Scintillators will be cured and post-processed with air interception. Others will use oxygen-purged resin material, and various types and contents of antioxidant agents will be tested. These modified new plastic scintillators will be evaluated and compared, with the purpose of realizing low-cost and stable materials.

Conflict of interest

Declarations of interest: none.

Acknowledgment

We wish to express our gratitude for the technical assistance of Mr. Hiroki Morii at Niigata University. This work was supported by JSPS KAKENHI [grant numbers 19340057, 23340063, 26800148, 17K18161, and 17K18316].

References

[1] T.K. Lewellen, Recent developments in PET detector technology, Physics in Medicine and Biology 53 (2008) R287-R317.

[2] L. Archambault, T.M. Briere, F. Pönisch, L. Beaulieu, D.A. Kuban, A. Lee, S. Beddar, Toward a real-time in vivo dosimetry system using plastic scintillation detectors, International Journal of

Radiation Oncology Biology Physics 78 (2010) 280-287.

[3] K. Deprez, R.V. Holen, S. Vandenberghe, A high resolution SPECT detector based on thin continuous LYSO, Physics in Medicine and Biology 59 (2014) 153-171.

[4] M. Košťál, J. Šoltés, L. Viererbl, Z. Matěj, F. Cvachovec, V. Rypar, E. Losa, Measurement of neutron spectra in a silicon filtered neutron beam using stilbene detectors at the LVR-15 research reactor, Applied Radiation and Isotopes 128 (2017) 41-48.

[5] R. Zboray, R. Adams, Z. Kis, Scintillator screen development for fast neutron radiography and tomography and its application at the beamline of the 10 MW BNC research reactor, Applied Radiation and Isotopes 140 (2018) 215-223.

[6] Y.-Y. Ji, H.-S. Chang, T. Lim, W. Lee, Application of a SrI_2(Eu) scintillation detector to in situ gamma-ray spectrometry in the environment, Radiation Measurements 122 (2019) 67-72.

[7] A. Pla-Dalmau, A.D. Bross, K.L. Mellott, Low-cost extruded plastic scintillator, Nuclear Instruments and Methods in Physics Research Section A 466 (2001) 482-491.

[8] A. Quaranta, S. Carturan, T. Marchi, M. Cinausero, C. Scian, V.L. Kravchuk, M. Degerlier, F. Gramegna, M. Poggi, G. Maggioni, Doping of polysiloxane rubbers for the production of organic scintillators, Optical Materials 32 (2010) 1317-1320.

[9] A. Mahl, H.A. Yemam, R. Fernando, J.T. Koubek, A. Sellinger, U. Greife, ^{10}B enriched plastic scintillators for application in thermal neutron detection, Nuclear Instruments and Methods in Physics Research Section A 880 (2018) 1-5.

[10] L. Ovechkina, K. Riley, S. Miller, Z. Bell, V. Nagarkar, Gadolinium loaded plastic scintillators for high efficiency neutron detection, Physics Procedia 2 (2009) 161-170.

[11] A. Quaranta, S. Carturan, T. Marchi, M. Buffa, M. Degerlier, M. Cinausero, G. Guastalla, F. Gramegna, G. Valotto, G. Maggioni, V.L. Kravchuk, Doped polysiloxane scintillators for thermal neutrons detection, Journal of Non-Crystalline Solids 357 (2011) 1921-1925.

[12] L.C. Alberich (ATLAS collaboration), ATLAS Tile Calorimeter performance with Run 1 data, Nuclear Instruments and Methods in Physics Research Section A 824 (2016) 12-14.

[13] The CDF II collaboration, The CDF II Detector Technical Design Report, Fermilab-Pub-96/390-E, 1996.

[14] H. Ono, H. Miyata, S. Iba, N. Nakajima, A.L.C. Sanchez, Y. Fujii, S. Itoh, F. Kajino, J. Kanzaki, K. Kawagoe, S. Kim, S. Kishimoto, T. Matsumoto, H. Matsunaga, A. Nagano, R. Nakamura, T. Takeshita, Y. Tamura, S. Yamauchi, Beam test results of a high-granularity tile/fiber electromagnetic calorimeter, Nuclear Instruments and Methods in Physics Research Section A 600 (2009) 398-407.

[15] Y. Kuroda, S. Oguri, Y. Kato, R. Nakata, Y. Inoue, C. Ito, M. Minowa, A mobile antineutrino detector with plastic scintillators, Nuclear Instruments and Methods in Physics Research Section A 690 (2012) 41-47.

[16] S. Oguri, Y. Kuroda, Y. Kato, R. Nakata, Y. Inoue, C. Ito, M. Minowa, Reactor antineutrino monitoring with a plastic scintillator array as a new safeguards method, Nuclear Instruments and Methods in Physics Research Section A 757 (2014) 33-39.

[17] I. Alekseev, V. Belov, V. Brudanin, M. Danilov, V. Egorov, D. Filosofov, M. Fomina, Z. Hons, S. Kazartsev, A. Kobyakin, A. Kuznetsov, I. Machikhiliyan, D. Medvedev, V. Nesterov, A. Olshevsky, D. Ponomarev, I. Rozova, N. Rumyantseva, V. Rusinov, A. Salamatin, Ye. Shevchik, M. Shirchenko, Yu. Shitov, N. Skrobova, A. Starostin, D. Svirida, E. Tarkovsky, I. Tikhomirov, J. Vlášek, I. Zhitnikov, D. Zinatulina, DANSS: Detector of the reactor antineutrino based on solid scintillator, arXiv:physics.ins-det/1606.02896v3.

[18] C. Aberle, C. Buck, F.X. Hartmann, S. Schönert, Light yield and energy transfer in a new Gd-loaded liquid scintillator, Chemical Physics Letters 516 (2011) 257-262.

[19] M. Katsumata, H. Miyata, N. Tamura, T. Kawasaki, Stability of Gd-loaded liquid scintillator for reactor neutrino detection, Nuclear Instruments and Methods in Physics Research Section A 629

(2011) 50-56.
[20] W. Beriguete, J. Cao, Y. Ding, S. Hans, K.M. Heeger, L. Hu, A. Huang, K.-B. Luk, I. Nemchenok, M. Qi, R. Rosero, H. Sun, R. Wang, Y. Wang, L. Wen, Y. Yang, M. Yeh, Z. Zhang, L. Zhou, Production of a gadolinium-loaded liquid scintillator for the Daya Bay reactor neutrino experiment, Nuclear Instruments and Methods in Physics Research Section A 763 (2014) 82-88.
[21] M. Watanabe, M. Katsumata, H. Ono, T. Suzuki, H. Miyata, Y. Itoh, K. Ishida, M. Tamura, Y. Yamaguchi, First performance test of newly developed plastic scintillator for radiation detection, Nuclear Instruments and Methods in Physics Research Section A 770 (2015) 197-202.
[22] Saint-Gobain Co., BC-408, BC-412, BC-416, available at https://www.crystals.saint-gobain.com/products/bc-408-bc-412-bc-416 (accessed on April 15th, 2019).
[23] P. Rossi, E. Polli, M. Albicocco, H. Avakian, N. Bianchi, G.P. Capitani, A. Deppman, E. De Sanctis, V. Giourdjian, P. Levi Sandri, S. Mansanta, M. Mirazita, V. Muccifora, A.R. Reolon, M. Taiuti, A. Rottura, M. Anghinolfi, M. Battaglieri, P. Corvisiero, E. Golovach, A. Longhi, V.I. Mokeev, M. Olcese, G. Ricco, M. Ripani, M. Sanzone, V. Sapunenko, R. Morandotti, Performance of the new plastic scintillator NE110A for the CLAS large angle calorimeter, Nuclear Instruments and Methods in Physics Research Section A 381 (1996) 32-38.
[24] M. Gierlik, T. Batsch, R. Marcinkowski, M. Moszyński, T. Sworobowicz, Light transport in long, plastic scintillators, Nuclear Instruments and Methods in Physics Research Section A 593 (2008) 426-430.

Figure Captions

Fig. 1. Experimental setup of the light yield and attenuation length measurement. For the attenuation length measurement, components that are fixed to motorized stage are moved every 1 cm. The scintillators and the PMT surface are both covered with black sheets to shield them from ambient light or from light emitted by either scintillator.
Fig. 2. Plastic scintillator samples measuring 40 mm × 75 mm × 3 mm. From left: BC408-1, NGT5-1, and NGT6-1.
Fig. 3. Pulse shapes of the sample plastic scintillators observed by oscilloscope: (a) BC408-1, (b) NGT1-1, (c) NGT2-1, (d) NGT3-1, (e) NGT4-1, (f) NGT5-1, and (g) NGT6-1. The irradiation position of the β-ray was located 6 cm from the PMT surface on the centerline in the length direction of the scintillator.
Fig. 4. ADC histograms of PH distribution of (a) BC408-1, (b) NGT1-1, (c) NGT2-1, (d) NGT3-1, (e) NGT4-1, (f) NGT5-1, and (g) NGT6-1 irradiated by β-rays. The horizontal axis of (a) uses a scale twice as large as that in the other figures.
Fig. 5. Long-term stability of the sample scintillators: (a) BC408, (b) NGT1, (c) NGT2, (d) NGT3, (e) NGT4, (f) NGT5, and (g) NGT6.
Fig. 6. Attenuation length results (^{90}Sr source distance from PMT surface versus mean value). (a) BC408L (day 0), (b) BC408L (day 365), (c) NGT6L-1 (day 33), (d) NGT6L-1 (day 280), (e) NGT6L-2 (day 33), (f) NGT6L-2 (day 280).
Fig. 7. Long-term attenuation length stability.

Table Captions

Table 1. Plastic scintillator samples for light yield testing.
Table 2. Light yields and thicknesses of new plastic scintillators and BC408. The irradiation position of the β-ray was located 6 cm from the PMT surface on the centerline in the length direction of the scintillator.
Table 3. Thickness of the sample scintillators, where Position *x* is the distance from the PMT surface and Av represents the average thickness.
Table 4. Storage times of sample scintillators before measurement and attenuation lengths obtained

by function fitting. For BC408L, days elapsed since the first measurement are given. For NGT6L-1,2, days elapsed since scintillator demolding are given.

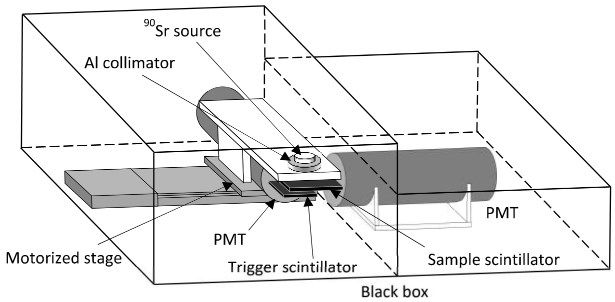

^{90}Sr source
Al collimator
PMT
Motorized stage
PMT
Trigger scintillator
Sample scintillator
Black box

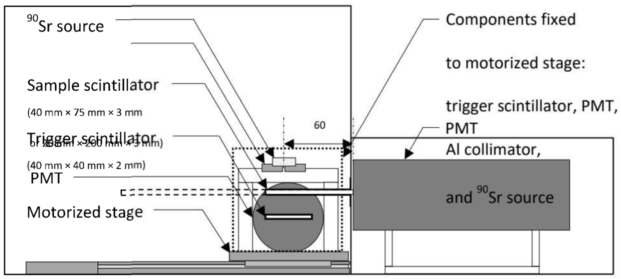

^{90}Sr source
Sample scintillator
(40 mm × 75 mm × 3 mm
Trigger scintillator
(40 mm × 40 mm × 2 mm)
PMT
Motorized stage
60
Components fixed
to motorized stage:
trigger scintillator, PMT,
PMT
Al collimator,
and ^{90}Sr source

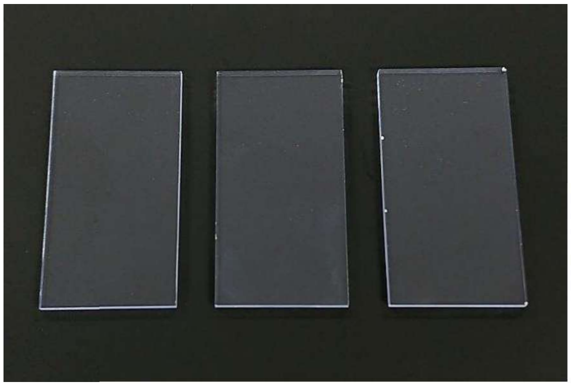

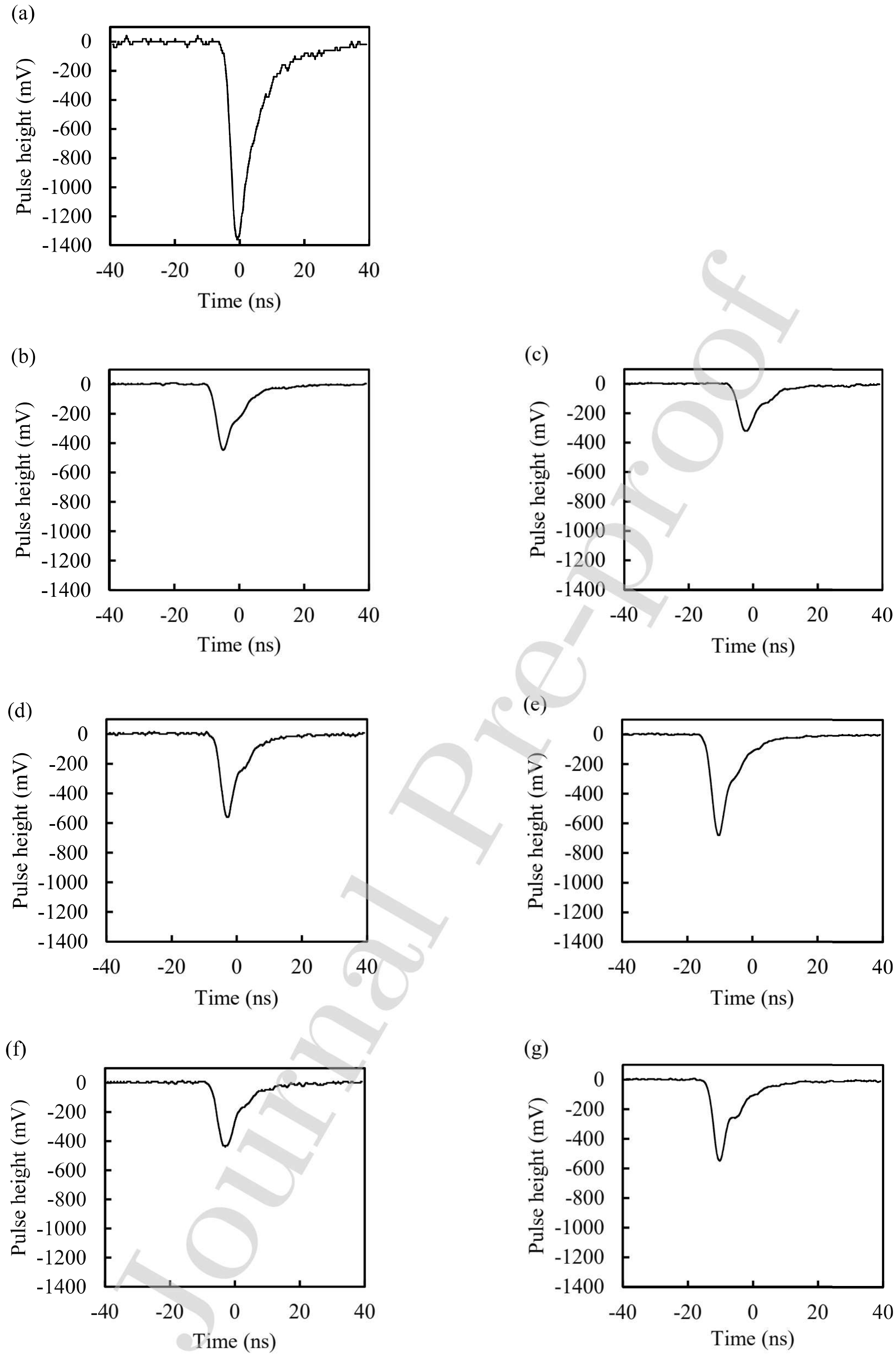

(a)
(b)
(c)
(d)
(e)
(f)
(g)
Pulse height (mV)
0
-200
-400
-600
-800
-1000
-1200
-1400
Time (ns)
-40
-20
0
20
40

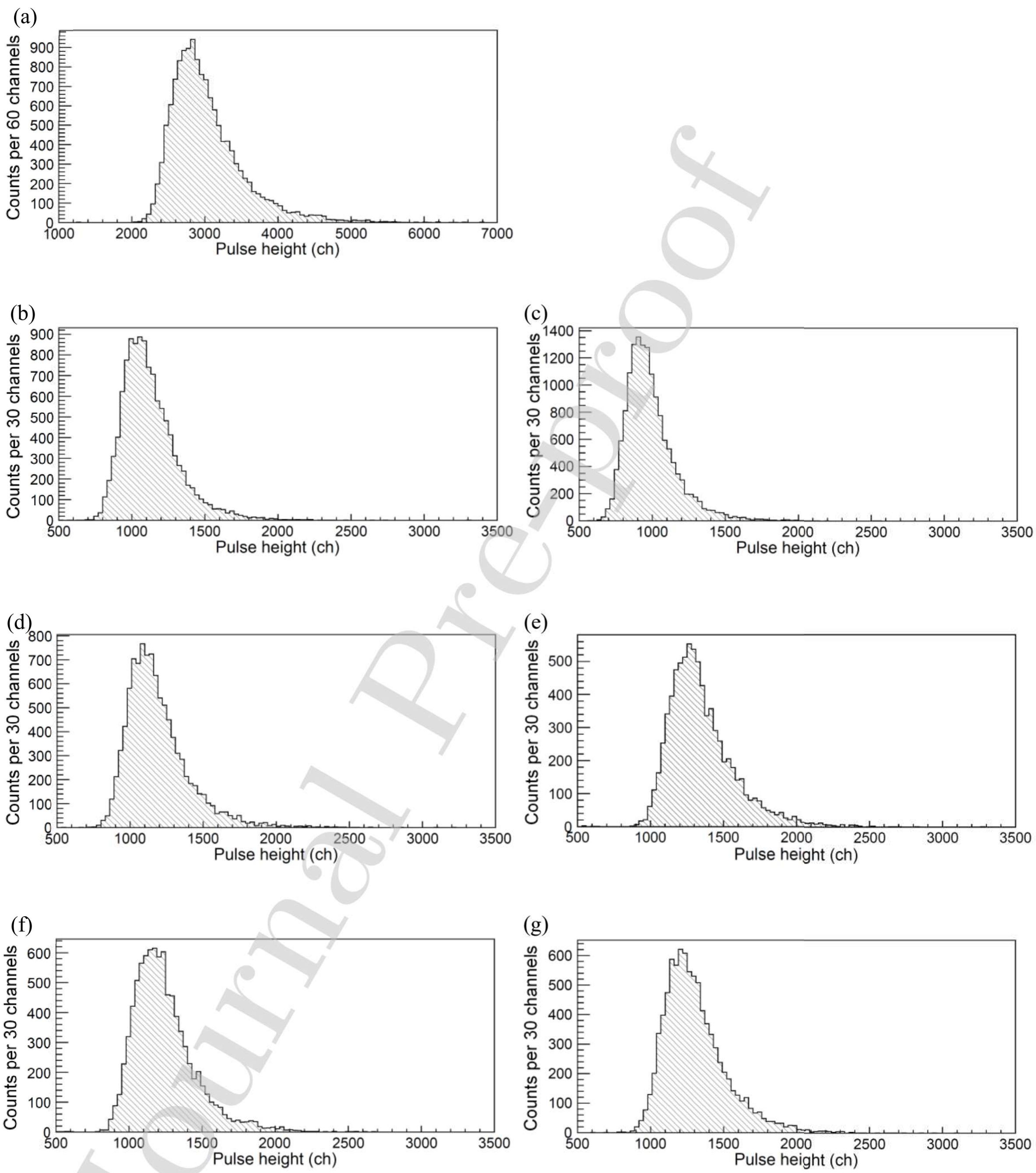
(a)
Counts per 60 channels
Pulse height (ch)
0 100 200 300 400 500 600 700 800 900
1000 2000 3000 4000 5000 6000 7000
(b)
Counts per 30 channels
Pulse height (ch)
0 100 200 300 400 500 600 700 800 900
500 1000 1500 2000 2500 3000 3500
(c)
Counts per 30 channels
Pulse height (ch)
0 200 400 600 800 1000 1200 1400
500 1000 1500 2000 2500 3000 3500
(d)
Counts per 30 channels
Pulse height (ch)
0 100 200 300 400 500 600 700 800
500 1000 1500 2000 2500 3000 3500
(e)
Counts per 30 channels
Pulse height (ch)
0 100 200 300 400 500
500 1000 1500 2000 2500 3000 3500
(f)
Counts per 30 channels
Pulse height (ch)
0 100 200 300 400 500 600
500 1000 1500 2000 2500 3000 3500
(g)
Counts per 30 channels
Pulse height (ch)
0 100 200 300 400 500 600
500 1000 1500 2000 2500 3000 3500

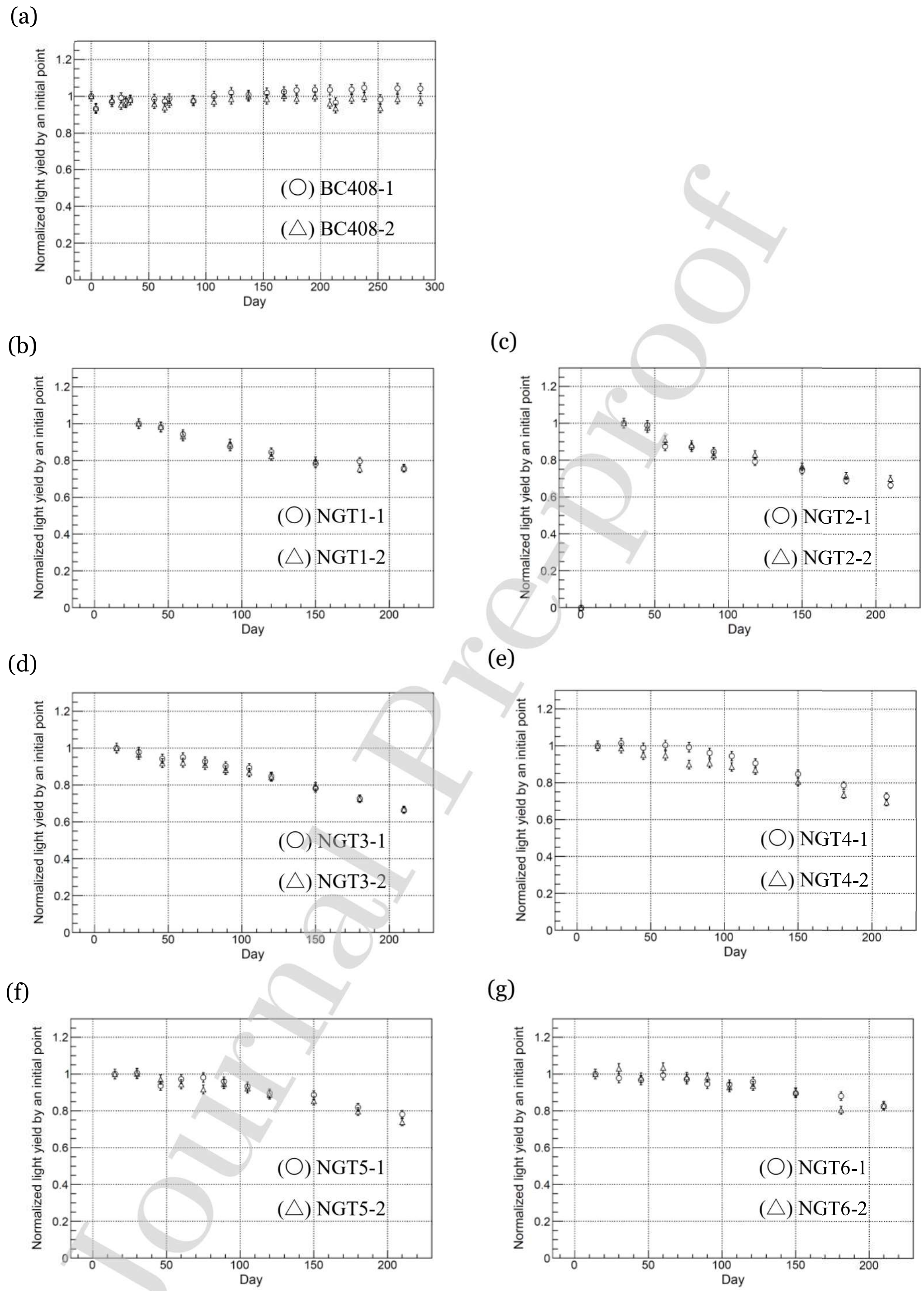
(a)
Normalized light yield by an initial point
Day
(○) BC408-1
(△) BC408-2
(b)
(○) NGT1-1
(△) NGT1-2
(c)
(○) NGT2-1
(△) NGT2-2
(d)
(○) NGT3-1
(△) NGT3-2
(e)
(○) NGT4-1
(△) NGT4-2
(f)
(○) NGT5-1
(△) NGT5-2
(g)
(○) NGT6-1
(△) NGT6-2

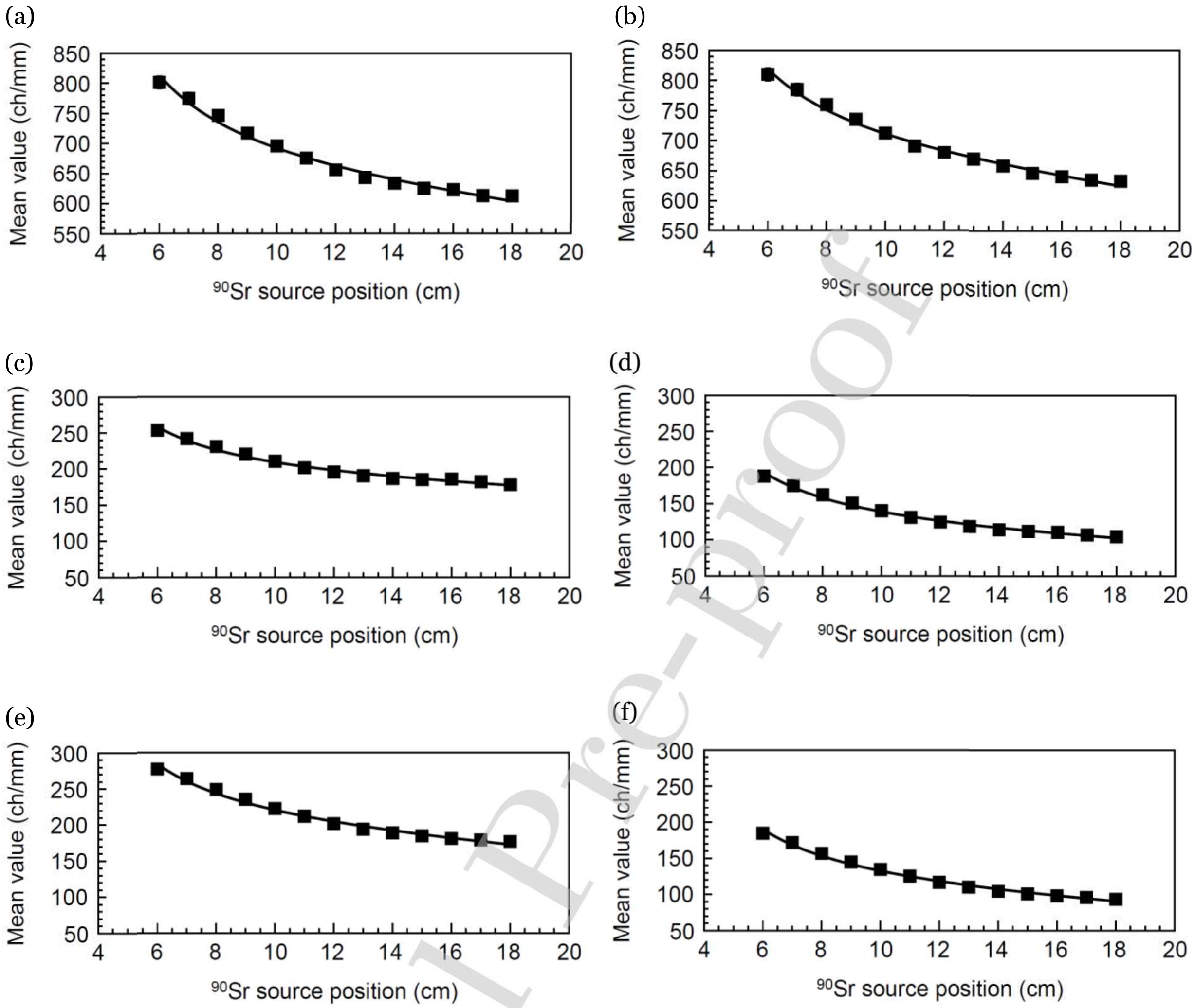
(a)
Mean value (ch/mm)
850
800
750
700
650
600
550
4
6
8
10
12
14
16
18
20
^{90}Sr source position (cm)
(b)
(c)
(d)
(e)
(f)
300
250
200
150
100
50

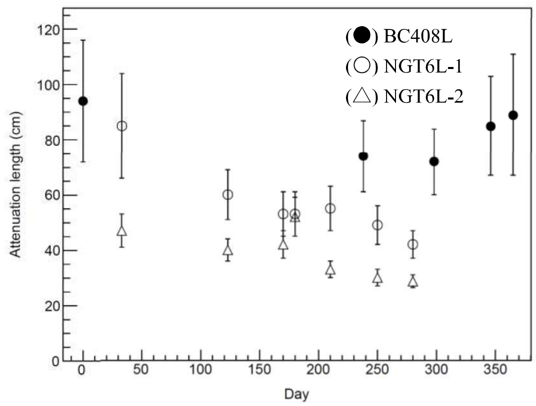
(●) BC408L
(○) NGT6L-1
(△) NGT6L-2
Attenuation length (cm)
Day
0
20
40
60
80
100
120
0
50
100
150
200
250
300
350

Sample name	BHT (wt%)	Post heating time (h)
NGT1-1, 2	0	0
NGT2-1, 2	0	6
NGT3-1, 2	0.1	0
NGT4-1, 2	0.1	6
NGT5-1, 2	1	0
NGT6-1, 2	1	6

Sample name		Normalized mean (ch/mm)	Mean value relative to BC408 (%)	Sample thickness (mm)
BC408	1	986 ±26	100 ±3	3.073
	2	988 ±26	100 ±3	3.116
NGT1	1	379 ±10	38 ±1	2.972
	2	372 ±10	38 ±1	2.955
NGT2	1	332 ± 9	34 ±1	2.973
	2	321 ± 8	33 ±1	3.052
NGT3	1	418 ±11	42 ±1	2.845
	2	452 ±12	46 ±1	2.977
NGT4	1	433 ±11	44 ±1	3.115
	2	417 ±11	42 ±1	3.094
NGT5	1	414 ±11	42 ±1	2.998
	2	396 ±10	40 ±1	3.093
NGT6	1	421 ±11	41 ±1	3.101
	2	405 ±11	42 ±1	2.990

Position x (cm)	BC408L (mm)	NGT6L-1 (mm)	NGT6L-2 (mm)
6	2.990	2.942	2.945
7	2.998	2.930	2.934
8	3.010	2.921	2.929
9	3.024	2.924	2.929
10	3.040	2.932	2.930
11	3.054	2.931	2.931
12	3.068	2.930	2.932
13	3.080	2.938	2.925
14	3.089	2.941	2.925
15	3.095	2.941	2.931
16	3.103	2.941	2.947
17	3.110	2.944	2.949
18	3.112	2.950	2.960
Av.	3.059	2.936	2.936

Sample name	Date of first measurement (days)	Date of last measurement (days)	Attenuation length of first measurement (cm)	Attenuation length of last measurement (cm)
BC408L	0	365	94 ± 22	89 ± 19
NGT6L-1	33	280	85 ± 19	42 ± 5
NGT6L-2	33	280	47 ± 6	29 ± 2